Available online at www.sciencedirect.com
SCIENCE DIRECT®

Polymer 45 (2004) 1815–1822

polymer

www.elsevier.com/locate/polymer

Syndiospecific polymerization of propene under different processes with different bridged [(RPh)$_2$C(Cp)(2,7-^{tert}BuFlu)]ZrCl$_2$ metallocene catalysts

Fabian Müller[a], Andreas Hopf[a], Walter Kaminsky[a,*], Piet Lemstra[b], Joachim Loos[b]

[a] *Institute for Technical and Macromolecular Chemistry, University of Hamburg, Bundesstr. 45, D-20146 Hamburg, Germany*
[b] *Dutch Polymer Institute, Department of Chemical Engineering, Eindhoven University of Technology, P.O. Box 513, 5600 Eindhoven, The Netherlands*

Received 25 August 2003; received in revised form 9 January 2004; accepted 12 January 2004

Abstract

The synthesis of syndiotactic polypropene was achieved by using new C_S-symmetric *ansa*-metallocene catalysts of the type [Ph$'_2$C(Cp)(2,7-^{tert}Bu$_2$Flu)]ZrCl$_2$ (Ph$'_2$ = Ph$_2$, (4-MePh)$_2$, 3,4$'$-Me$_2$Ph$_2$, (4-OCH$_3$Ph)$_2$). Applying these catalysts, the influence of the substitution pattern of the bridge on the polymerization performance can be studied and highly syndiotactic polypropene (*rrrr* > 99%) with high molar masses ($M_\eta > 10^6$ g/mol) and high melting temperatures (up to 153 °C) was obtained.

Propene was polymerized at different temperatures under four sets of conditions: in toluene solution, bulk, toluene slurry, and gas phase with NaCl as stirred bed material. Methylaluminoxane (MAO) and methylaluminoxane supported on silicagel (MAO/SiO$_2$) were used as cocatalyst, respectively. In order to estimate the influence of the process on the single site properties of the catalysts, comparisons were made between polymer properties, i.e. microstructure, melting temperature, molar mass, and polymer morphology, thus allowing the effect of the support on the catalyst to be observed.

Keywords: Syndiotactic polypropene; Metallocene; Methylaluminoxane

---

1. Introduction

The syndiospecific polymerization of propene to syndiotactic polypropene (sPP) by enantiomorphic site control mechanism has been enabled by the development of C_S-symmetric metallocene catalysts providing well-defined microstructures that are not readily obtained with heterogeneous Ziegler–Natta catalysts [1,2]. The first suitable spp-catalyst was synthesized by Ewen and Razavi in 1988 [3]. The two coordination sites are enantiotopic resulting in alternating enantiofacial orientations of the successive olefin insertions. Several modifications of Ewen's original catalyst design have been reported in literature [4]. By modifying the bridge (e.g. Ph$_2$C) higher molar masses of the produced polymers have been obtained [5], whereas the syndiotacticity has been increased by expansion of the fluorenyl ligand framework [6]. A substitution in 2 and 7 position with ^{tert}butyl groups has turned out to be very promising [7,8]. The influence of a modified Ph$_2$C bridge, which is substituted with electron withdrawing alkyl or alkoxy groups, on syndiotacticity, catalyst activity, and molar mass will be investigated in the present study.

Due to a totally new quality profile with some interesting features such as high transparency, high γ-resitance, high impact resistance, and a silky touch, sPP opens up niche markets, e.g. in the area of medical and cosmetic applications [9]. However, for an efficient application of metallocene catalysts in modern suspension or gas phase polymerization processes (*drop-in technology*) they have to be supported on carrier materials [10,11,12]. By applying these particle-forming processes, it is possible to prevent the polymer particles from sticking together and to the walls of the reactor (*reactor fouling*), because the catalyst serves as a template for polymer particle growth [13,14]. Among the variety of carriers, silica appeared to be a reasonable support because it possesses high surface area and porosity, has good mechanical properties, and is stable and inert under

---

[*] Corresponding author. Tel.: +49-40-42-83-83-162; fax: +49-40-42-83-86-008.

E-mail address: kaminsky@chemie.uni-hamburg.de (W. Kaminsky).

0032-3861/$ - see front matter © 2004 Elsevier Ltd. All rights reserved.
doi:10.1016/j.polymer.2004.01.029

polymerization and processing conditions [15]. Furthermore, the immobilization of metallocene complexes on a support should provide the possibility to reduce the amount of MAO [16]. Considering its high cost, this would be preferred. Among the several different methods [11,17] to prepare immobilized aluminoxane-based catalyst systems the method of indirect heterogenization of the metallocene on a with MAO pretreated silica proved to be favorably and was chosen in the present work.

In this paper, we report on the homogeneous and heterogeneous polymerization of propene with four highly active C_S-symmetric metallocenes combined with MAO and MAO/SiO_2 as cocatalyst, respectively.

2. Experimental

All procedures were performed under argon using Schlenk techniques.

2.1. Materials

Argon was purchased from Linde and purified by passing through a Messer Griesheim Oxisorp cartridge. Methylaluminoxane (MAO, 10 wt% toluene solution) and MAO-modified silica (MAO/SiO_2, 23 wt% Al) were purchased from Witco. After filtration of the commercial solution MAO was obtained by removal of toluene and residual TMA under vacuum. Propene (Messer Griesheim) and toluene (Merck) were purified by passing through columns with Cu catalyst (BASF R3-11) and molecular sieve 3 Å. Tri*iso*butylaluminium (TIBA) was purchased from Aldrich and employed without further purification. NaCl was purchased from Merck and dried in a drying oven for several days at 150 °C before use. Syntheses of complexes **1**–**4** (see Chart 1) were performed according to the general procedure reported in Ref. [7].

2.2. Preparation of supported catalysts

Applying procedure slurry and gas phase, the metallocenes were supported externally shortly before being introduced into the reactor For the standard heterogenization, 1 ml of a 2×10^{-3} molar toluenic solution of the metallocene was added to 4.5 ml of a toluenic suspension of MAO/SiO_2 (100 mg/ml). The resulting Al/Zr ratio, in relation to the Al on the support, was therefore 2000. The mixture was allowed to stir at room temperature for 10 min and was then introduced into the reactor by a gas tight syringe.

2.3. Polymerization reactions

The polymerization conditions are summarized in Table 1 for each process.

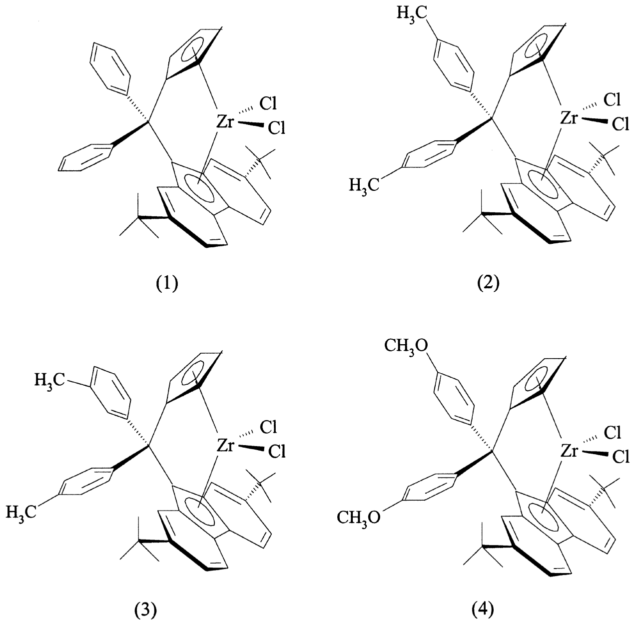

(1) (2) (3) (4)

Chart 1. Catalysts used.

Procedures A and C. Polymerizations were carried out in a 1 l Büchi AG laboratory autoclave with type I glass pressure vessel equipped with an additional internal cooling system. Monomer feed of the gaseous monomer was maintained with a Peteric 3002 pressflow controller. The reaction was monitored by a Büchi Data System bds 488. For the standard experiment, the reactor was evacuated at 95 °C for 1 h, flushed several times with argon and charged subsequently with 200 ml toluene and the desired amount of MAO or TIBA, respectively. Propene was added so that the monomer concentration was 1.38 mol/l. Polymerization was started by addition of toluenic metallocene solution or a toluenic suspension of the heterogenized metallocene, respectively. During the reaction, the total pressure was kept constant by supplying propene. Polymerization was quenched by injection of 5 ml of ethanol. The content of the reactor was stirred overnight with dilute hydrochloric acid followed by neutralization with $NaHCO_3$, washing with water, filtered off and dried under vacuum at 60 °C until the weight remained constant.

Procedure B. Polymerizations were carried out in a 500 ml Büchi AG type I steel autoclave. During the polymerization propene was not constantly added. The reaction was performed in such a way that the monomer conversion remained below 10%. For the standard experiment, the reactor was evacuated at 95 °C for 1 h, flushed several times with argon and charged with MAO. The reactor was cooled to -20 °C and propene was added so that the reactor was filled with 375 ml of liquid monomer. The reactor was then heated to the desired polymerization temperature. Polymerization was started by addition of toluenic metallocene solution and quenched by injection of 5 ml of ethanol. Propene was allowed to evaporate and the residue was washed out of the reactor with toluene. Dilute hydrochloric acid was added and the resulting suspension

Table 1
Reaction conditions

Process	Reaction medium	Catalyst	Cocatalyst	Scavenger	Polymerization temperature (°C)	Monomer concentration (mol/l)
Solution (A)	Toluene 200 ml	**1**, **2**, **3**, **4** 5×10^{-7}–4×10^{-6} mol	MAO 200–650 mg	–	0–60	1.38
Bulk (B)	liquid propene 375 ml	**1**, **2**, **3** 1×10^{-6}–3×10^{-6} mol	MAO 600–1000 mg	–	−20–60	10.78–12.94
Slurry (C)	toluene 200 ml	**1**, **2**, **4** 1×10^{-6}–2×10^{-6} mol	MAO/SiO_2 225–450 mg	TIBA 1.0×10^{-3} mol	0–60	1.38
Gas phase (D)	NaCl 200 ml	**1**, **2**, **4** 2×10^{-6}–4×10^{-6} mol	MAO/SiO_2 450–900 mg	TIBA 1.2×10^{-3} mol	0–60	0.20–0.25

was allowed to stir overnight. The work-up steps were the same as for procedures A and C.

Procedure D. Polymerizations were carried out in a 2 l Büchi AG type II autoclave equipped with a helical stirrer. Monomer feed of propene was maintained with a Brooks TR 5850 mass flow controller; the reaction pressure was kept constant and the consumption of propene was monitored by a Simatic S5 unit from Siemens. For the standard experiment, the reactor was filled with 200 ml of pre-dried NaCl (250 g) and evacuated at 95 °C for 1.5 h while stirring (100 rpm). The reactor bed medium was treated with a toluenic solution of TIBA (2 ml of a 0.6 mol/l solution) 30 min prior to introduction of the heterogenized metallocene. After introduction of the catalyst, the reactor was evacuated for 10 min while stirring (200 rpm) in order to evaporate the surplus toluene. The reaction was started by fast pressurization (ca. 10 s) of the reactor with the monomer gas and starting the stirrer (200 rpm). The reaction was terminated by depressurization followed by short evacuation of the reactor and finally injection of 5 ml of ethanol. The reactor content was washed out with water and ethanol. Dilute hydrochloride was added and the mixture was allowed to stir overnight. The mixture was filtered and the precipitate was washed several times with $NaHCO_3$ solution, water and ethanol and finally dried in a vacuum oven at 60 °C.

2.4. Analytical procedures

^{13}C NMR spectra were recorded on a Bruker Ultrashield 400 spectrometer Polymer samples were measured at 100.62 MHz and 100 °C using 200–300 mg of polymer in 2.7 ml of hexachloro-1,3-butadiene and 0.3 ml of 1,1,2,2 tetrachloroethane-d_2 (1200 scans, 5 s delay time). Differential scanning calorimetry curves were recorded on a Mettler Toledo DSC 821^e instrument calibrated with *n*-heptane, mercury, gallium, indium, and zinc. Results of the second thermal cycle are presented exclusively. Viscosimetric measurements were performed in decahydronaphthalene at 135 °C using an Ubbelohde viscosimeter (0a capillary, $K = 0.005\ \mathrm{mm}^2\ \mathrm{s}^{-2}$). Mark–Houwing constants were taken from literature. Morphological investigations of the as prepared polymers were performed using a Fei Company environmental scanning electron microscope XL30 ESEM-FEG, which is equipped with a field emission electron source, using low voltage mode and a secondary electron detector. All SEM images shown here were recorded without additional sample pretreatment (e.g. surface etching, conductive coating).

3. Results and discussion

3.1. Activities

All catalysts were shown to be dependent on the polymerization temperature as well as on the polymerization process (see Table 2). The influence of the temperature on the catalyst activity was evaluated at 0, 15, 30, 45, and 60 °C for method A, C, and D and −20, −10, 0, 30, and 60 °C for bulk polymerizations, respectively. Generally, the observed activities yielded with these catalysts are among the highest values reported ever for the production of syndiotactic polypropene [5]. Particularly, employing the catalysts in the slurry procedure excellent activities are yielded compared to other studies [18] (6220 $\mathrm{kg_{polymer}/(mol_{Zr}\ h\ mol/l_{propene})}$ at 60 °C with catalyst **2**). By supporting the metallocene an exceptionally small decrease in catalyst activity is observed.

Fig. 1 shows the dependence of the polymerization process and polymerization temperature on the catalyst activity for catalyst **1**. It is worth mentioning that due to a better comparison of the processes, the catalyst activities reported in this paper are related to the monomer concentration. In the case of gas phase polymerizations, the highest activity was attained at 30 °C, decreasing at higher temperatures. On the other hand, employing the other processes, catalyst activity increases from −20 to 60 °C without showing any deactivation of the catalytic species. Due to avoidance of bimolecular deactivation, higher stability is expected for supported catalysts. Therefore, the course of catalyst activity in the gas phase process seems to be surprising at first sight. Nevertheless, it could be explained by monomer sorption effects. The polymerization of olefins over solid catalysts is a complex reaction, involving both physical and kinetic effects [19,20]. Monomer sorption plays a key role in determining the local monomer concentration at the active site [21]. The extent of sorption decreases as polymerization temperature increases. For this reason, decreased activity in gas phase polymerizations could be traced to the lower monomer concentration at the active site, reminding that only the bulk concentration of propene was kept constant in this procedure.

Two different bridges are compared in Fig. 2 by estimating the influence of the catalyst structure on the activity. Obviously, methyl substitution in the Ph_2C-bridge (catalyst **2**) leads to higher activities. However, the thermal stability of complex **2** is reduced since the maximum of catalyst activity is observed at 45 °C. Activities of the supported metallocene are approximately constant for

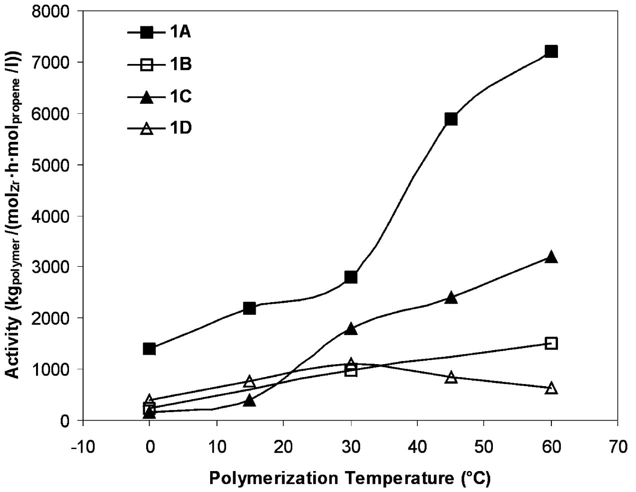

Fig. 1. Dependence of polymerization activity on polymerization process and temperature, catalyst **1**, all four processes.

Table 2
Activity in propene polymerization

Catalyst	T_p[a]	Activity ($\mathrm{kg_{polymer}/(mol_{Zr}\ h\ mol/l_{propene})}$)			
		A	B	C	D
1	−20		90		
	−10		180		
	0	1400	240	150	400
	15	2200		390	760
	30	2800	990	1800	1100
	45	5900		2400	840
	60	7200	1500	3200	640
2	−20		370		
	−10		430		
	0	1800	640	170	260
	15	3200		550	700
	30	5200	1100	3100	940
	45	11000		6400	550
	60	9600	3100	6200	470
3	0	600		90	580
	15	1400		420	600
	30	7000		2100	830
	45	4800		3600	680
	60	3200		5200	450
4	−20		30		
	−10		40		
	0	210	40		
	15	1200			
	30	6900	270		
	45	12400			
	60	7300	880		

[a] Polymerization temperature.

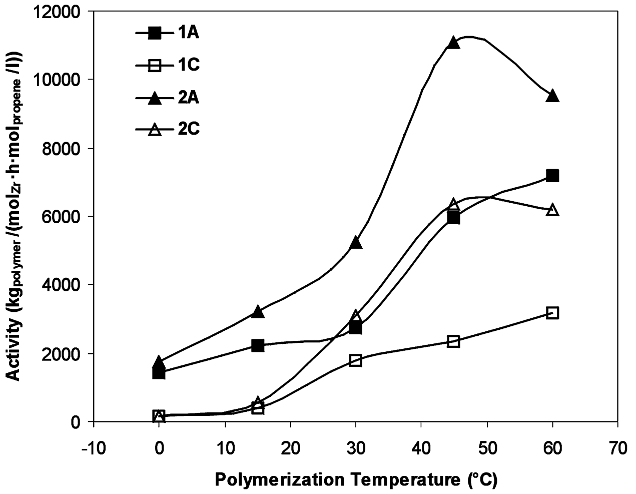

Fig. 2. Dependence of polymerization activity on polymerization process and temperature, catalyst **1** and **2**, solution (A) and slurry (C) process.

higher temperatures. Complexes **3** and **4** were shown to behave similar to complex **2**.

By plotting the logarithm of the activity versus $1/T$, the activation energies (E_a) can be calculated. For all catalysts, values around 25 kJ/mol were usually detected in cases of procedures A, B, and D, whereas the calculation of E_a for the process in slurry (C) was different. E_a was quantified to be nearly two times as large at temperatures between 0 and 30 °C. In the range between 30 and 60 °C, it was determined to be about 16 kJ/mol. This behaviour is supposed to be traced to diffusion- and prepolymerization effects, respectively [19].

3.2. Microstructure

Highly stereoregular syndiotactic polypropene is obtained with the catalyst systems used in this study reaching stereoregularities of $rrrr = 99\%$ and melting temperatures of 153 °C (see Table 3).

Analysis of the polymers by ^{13}C NMR spectroscopy gives an insight in the polymerization mechanism. The pentad distribution analysis of the ^{13}C NMR spectrum of the polymers produced in the processes A–D confirms the presence of *mm* stereodefects as the predominant source of stereo irregularity in the polymer microstructure as shown in Table 4. This is in accordance to an enantiomorphic site control mechanism [22], whereas the origin of the less frequent isolated *m* stereodefects are caused by a chain end control mechanism or an enantiomorphic site control mechanism where site epimerization, i.e. chain migration without insertion, or two sequential insertion errors such as site epimerization followed by chain epimerization occur. An increase of the monomer concentration in the propene polymerization with catalyst **1** in solution leads to an increase of the *rrrr* pentad and a decrease of the *rrrm* pentad whereas the *mm* stereodefects are hardly influenced [7]. This behaviour is most consistent with an enantiomorphic site control mechanism since one would not expect a concentration dependence on the stereospecifity for a chain end control mechanism. Because the value of the *mm* stereodefects is almost unchanged and the *m* stereoerrors disappeared with increasing monomer concentration, i.e. an increase in stereoselectivity, it is understandable that the primary source of *m* stereoerrors is due to isomerization of the site prior to monomer insertion (back skips). However, regioerrors are below the detection limit of the ^{13}C NMR analysis.

The microstructure of the produced polypropenes strongly depends on the polymerization temperature as well as on the applied polymerization process as shown in Fig. 3 for catalyst **2**. The highest degree of stereoselectivity, i.e. the highest value for the *rrrr* pentad, is obtained for the

Table 3
Polymerization results

Catalyst	T_p[a]	Molar mass (× 10^3 g/mol)				T_m (°C)				*rrrr* (%)			
		A	B	C	D	A	B	C	D	A	B	C	D
1	−20		1090				150				99		
	−10		1780				150				95		
	0	800	780	720	470	148	149	145	139	96	95	95	92
	15	500		500	350	149		143	143	96		93	94
	30	500	620	420	170	141	143	137	117	94	92	93	78
	45	300		290	90	137		132	103	88		94	56
	60	240	280	190	60	127	132	126	Amorphous	84	92	83	38
2	−20		1210				144				93		
	−10		1150				148				93		
	0	770	1380	780	560	146	145	142	140	95	98	93	88
	15	600		610	290	145		143	139	94		92	88
	30	430	760	470	140	137	140	139	121	93	94	92	82
	45	310		340	110	131		131	Amorphous	87	89	48	
	60	210	390	190	100	122	124	120	Amorphous	81	92	84	34
3	0	680		350	340	153		148	144	95		88	95
	15	540		470	360	151		142	143	94		86	94
	30	390		400	130	144		137	118	92		90	82
	45	270		280	110	133		129	Amorphous	88	87	62	
	60	250		190	80	123		118	Amorphous	84	84	42	
4	−20		610				129				80		
	−10		1060				133				84		
	0	340	860			140	128			86	83		
	15	330				142				86			
	30	280	430			141	123			84	76		
	45	220				136				85			
	60	130	190			129	120			78	67		

[a] Polymerization temperature

Table 4
Pentad distributions (in %) for catalyst 2, 30 °C

Process	*Mmmm*	*mmmr*	*rmmr*	*mmrr*	*mrmm* + *rmrr*	*mrmr*	*Rrrr*	*rrrm*	*mrrm*
A	0	0	0,9	2,2	1,0	0	92,7	3,2	0
B	0	0	0,8	2,0	1,1	0	93,8	2,3	0
C	0	0	1,0	2,1	1,2	0,5	91,7	3,4	0
D	0	0	1,8	4,2	3,3	0,1	81,6	8,9	0

bulk polymerization. At a polymerization temperature of 0 °C a fairly high stereoregularity (*rrrr* = 98%) is accomplished, slightly decreasing with increasing temperature. Applying process A and C, the polymers are less stereoregular. At 0 °C, the produced polypropenes show a syndiotacticity of 95% (A) and 93% (C), respectively. Again the *rrrr* values decrease with increasing polymerization temperature. This decline is more distinctive regarding the gas phase process (D). For this process the syndiotactic pentad content decreases from 88% at a polymerization temperature of 0 °C to 34% at 60 °C. Thus, for each process the highest stereoregularity is obtained for polymers produced at low polymerization temperatures, which is in accordance with an enantiomorphic site control mechanism. The dependence of the polymerization process on the stereoregularity can be interpreted by the role of the monomer concentration. Polymerizing in liquid propene (B) the monomer concentration is about 9 times higher than applying process A or C. In gas phase polymerizations, the monomer concentration constitutes only 2% of that (see Table 1). This decrease in monomer concentration results in an increase of stereodefects leading to a lower stereoselectivity.

Apparently, the structure of the bridge affects the stereoselectivity to a minor degree (see Table 3). As with catalyst **1**, **2**, and **3** comparable syndiotactic pentad contents are obtained, catalyst **4** shows a peculiar polymerization behavior in terms of selectivity. The stereoregularity is lower compared to the other systems, but hardly not influenced by the polymerization temperature. A decrease in selectivity is observed only at a temperature of 60 °C. Probably, the methoxy substitution of structure **4** allows an intermolecular complexation leading to lower stereoselectivities.

As a result of the low content of stereodefects high melting temperatures can be observed. As shown in Table 3 polymers with a melting temperature up to 153 °C can be obtained. Due to the high content of stereo errors, polymerizations in the gas phase process (D) yield in amorphous polymers at higher polymerization temperatures. Basically the melting temperatures correlate with the syndiotacticity, i.e. the higher the *rrrr* pentad content the higher the melting temperature. However, small deviations can be observed in this relationship. For example in process B with catalyst **1**, the melting temperatures at −20 and −10 °C are determined to be 150 °C although the polymers differ from *rrrr* values (99 and 95%, respectively). This might be explained by a different distribution of stereodefects along the polymer chain [23,24].

3.3. Molar masses

The molar masses, determined by viscosimetry, are summarised in Table 3. They cover a wide scope, from 59,000 to 1,780,000 g/mol. Apparently, the structure of the metallocene has no great influence on the molar mass of the produced polypropylenes. Examplary, the dependence of the molar mass on the polymerization temperature and

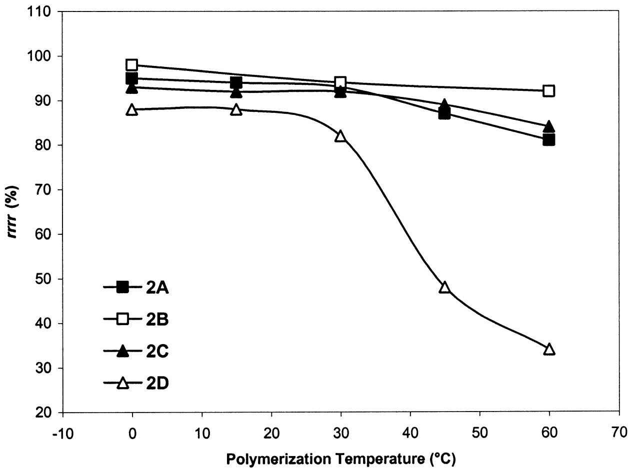

Fig. 3. Dependence of syndiotacticity (*rrrr* pentad content) on polymerization process and temperature, catalyst **2**, all four processes.

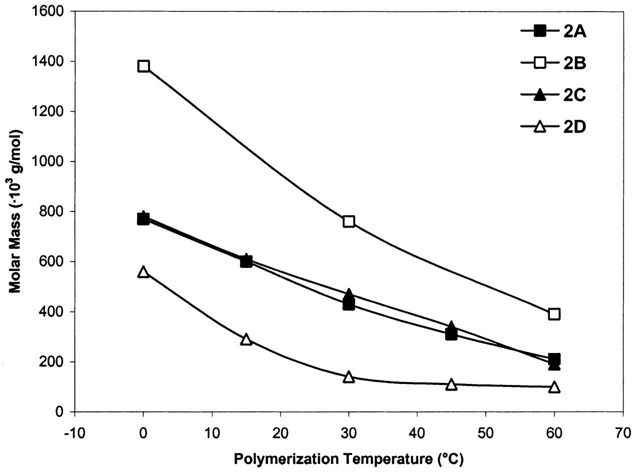

Fig. 4. Dependence of molar mass on polymerization process and temperature, catalyst **2**, all four processes.

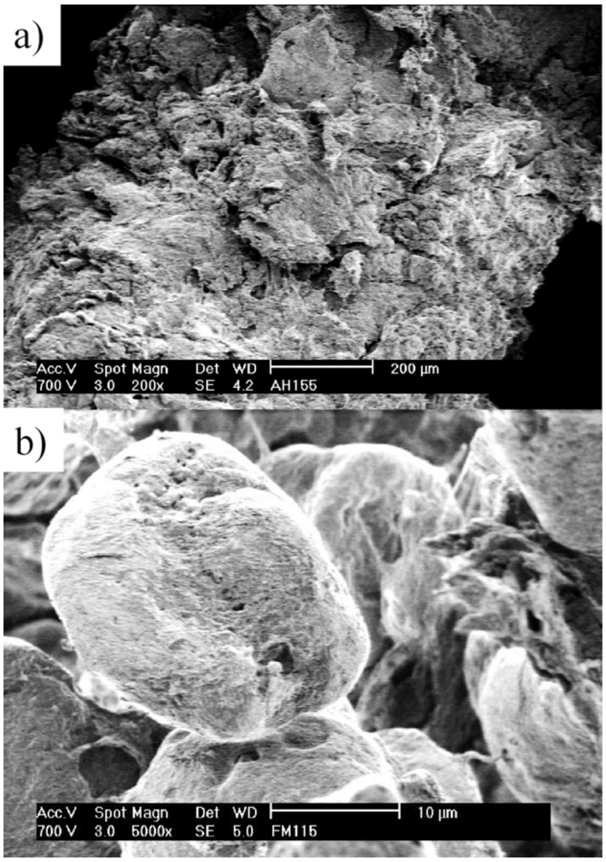

Fig. 5. (a) SEM image of sPP produced by catalyst **2** in solution (A) at 60 °C, 200 times magnified and (b) SEM image of sPP produced by catalyst **2** in gas phase (D) at 60 °C, 5,000 times magnified.

process is presented for catalyst **2** in Fig. 4. For every process, the highest molar masses are obtained for polymers produced at low polymerization temperatures. By raising the polymerization temperature, an increase in chain termination reactions leads to decreased molar masses. The effect of the polymerization process on the molar masses is also obvious. The molar masses of polypropenes produced with procedure B are 2 times higher than those of the products obtained with the methods A and C, which produce similar molar masses. By applying procedure D, the molar masses are effectively halved comparing to methods A and C. Again this behaviour could be explained by consideration of the monomer concentration. As mentioned above the monomer concentration using process A and C is distinctly lower than using process B. In gas phase polymerizations (D), propene concentration is still lower. The lack of monomer at the active site will facilitate chain termination reactions such as β-hydride elimination. For this reason the dependence of molar masses of the polymers reflects the local monomer concentration in each process. An influence of the support can be excluded as the polypropylenes produced in heterogeneous polymerizations C have similar molar masses as the products when employing the homogenous process A.

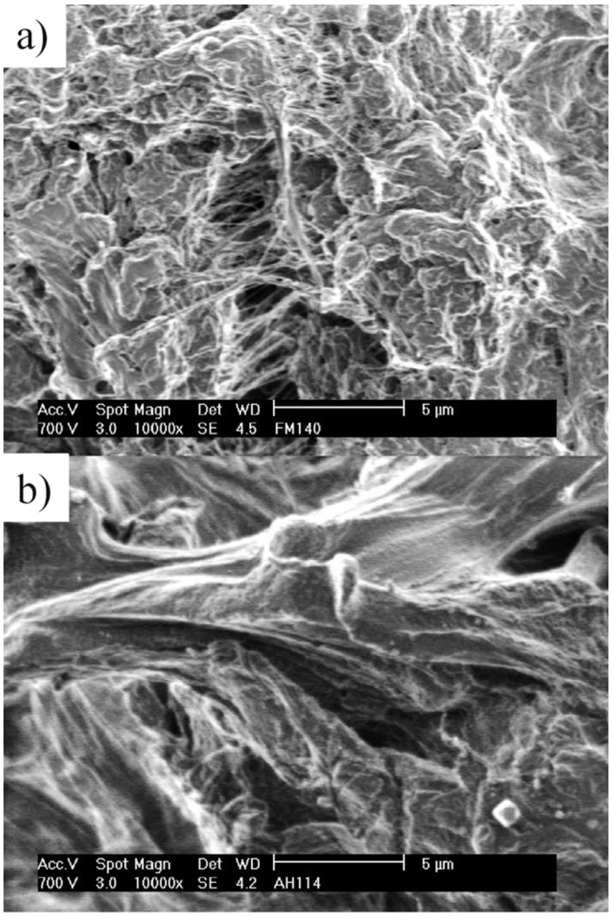

Fig. 6. (a) SEM image of sPP produced by catalyst **2** in slurry (C) at 60 °C, 10,000 times magnified and (b) SEM image of sPP produced by catalyst **2** in bulk (B) at 60 °C, 10,000 times magnified.

3.4. Morphology

After polymerization and drying, the morphology of the polymer products has been investigated using the technique of scanning electron microscopy. Both, the overall particle morphology as well as the local organization imaged at high-resolution conditions differ significantly with applied polymerization conditions. In the case of polymerization in toluene, the polymer product appearance is fluffy and is independent of the used polymerization conditions and reaction type (solution or slurry). As an example, Fig. 5(a) shows part of an sPP flake polymerized in solution at 60 °C. In contrast, heterogeneous polymerization D results in sufficient replication of the initial catalyst to form powder morphology (Fig. 5(b)).

High-resolution SEM images show more details of the internal morphology of the polymer products. In the case of polymerization in solution or slurry, the local appearance of the powder products is rather diverse: next to region of dense polymer, tiny filament-like polymer fibrils are visible (Fig. 6(a), slurry polymerization). The formation of these fibrils can be explained by local shear stresses present during the polymerization process. On the other hand, polymer products prepared in liquid propene (B) show a high bulk density and less local deformation (Fig. 6(b)).

In general, the catalyst structure has no influence on the polymer morphology. Only the applied polymerization conditions, e.g. reactor type and the type of catalyst used, homogeneous or heterogeneous, determine the product morphology.

4. Conclusions

With the use of C_S-symmetric catalysts, in which the fluorenyl ligand is substituted in 2,7-position, it is possible to produce highly syndiotactic polypropene with fairly high activities. As the substitution of the bridge does not significantly influence the polymerization performance, the effects observed in propene polymerization were found to be strongly dependent on the applied polymerization process and temperature. But the polymerization behavior is not so much the result of the supporting itself, as an effect of the monomer concentration. By polymerizing in liquid propene (B), the monomer concentration is higher than applying process A or C. In gas phase polymerizations (D), the monomer concentration again decreases noticeable. This decrease in monomer concentration results in an increase of stereo errors and decrease of molar masses. Increasing polymerization temperature is found to result in increased activity and decreased molar mass and stereoselectivity. By employing the supported catalyst, a replication of the carrier material was found to be observed in the gas phase process (D).

References

[1] Brintzinger HH, Fischer D, Mülhaupt R, Rieger B, Waymouth R. Angew Chem 1995;107:1255–83.

[2] Kaminsky W, Arndt M. Adv Polym Sci; 127, 143–187.

[3] Ewen JA, Jones RL, Razavi A. J Am Chem Soc 1988;110:6255.

[4] Coates GW. Chem Rev 2000;100:1223–52.

[5] Resconi L, Cavallo L, Fait A, Piemontesi F. Chem Rev 2000;100: 1253–345.

[6] Miller SA, Bercaw JE. Abstr Am Chem Soc 1999;217:151-INOR. US 6,469,188.

[7] Hopf A, Kaminsky W. Catal Commun 2002;3:459–64.

[8] Shiomura T, Kohno M, Inoue N, Yokote Y, Akiyama M, Asanuma T, Sugimoto R, Kimura S, Abe M. Stud Surf Sci Catal 1994;89:327–38.

[9] Mühlhaupt R. Macromol Chem Phys 2003;204:289–327.

[10] Kristen MO. Top Catal 1999;7:89.

[11] Hlatky GG. Chem Rev 2000;100:1347–76.

[12] Karol FJ. Macromol Symp 1995;89:563.

[13] Ray H, Han-Adebekun GC. J Appl Polym Sci 1997;65:1037.

[14] Boor J. Ziegler–Natta catalysts and polymerizations. New York: Academic; 1979.

[15] Fink G, Steinmetz B, Zechlin J, Przybyla C, Tesche B. Chem Rev 2000;100:1377–90.

[16] Chien JCW, Wang BP. J Polym Sci, A 1988;26:3089.

[17] Carnahan EM, Jacobsen GB. CATTECH 2000;4:74–88.

[18] Chunming C, Wei C, Chunyan S, Zhenhua J, Xiaoyu H. Acta Petrolei Sinica 1997;10:56–61.

[19] Zechlin J, Steinmetz B, Tesche B, Fink G. Macromol Chem Phys 2000;201:515–24.

[20] Meier GB, Weickert G, van Swaaij WPM. J Appl Polym Sci 2001;81: 1193–206.

[21] Hutchinson RA, Ray WH. J Appl Polym Sci 1990;41:51–81.

[22] Busico V, Cipullo R. Prog Polym Sci 2001;26:443–533.

[23] Loos J, Schauwienold AM, Yan S, Petermann J, Kaminsky W. Polym Bull 1997;38:185–9.

[24] Loos J, Buhk M, Petermann J, Zoumis K, Kaminsky W. Polymer 1996;37:387–91.